The Astrophysical Journal, 678:1230–1236, 2008 May 10

ON THE NATURE OF THE VARIABILITY POWER DECAY TOWARD SOFT SPECTRAL STATES IN X-RAY BINARIES: CASE STUDY IN CYGNUS X-1

Lev Titarchuk[1,2,3] and Nikolai Shaposhnikov[4]

Received 2007 August 2; accepted 2008 February 3

ABSTRACT

A characteristic feature of the Fourier power density spectrum (PDS) observed from black hole X-ray binaries in low/hard and intermediate spectral states is a broadband-limited noise characterized by a constant below some frequency (a "break" frequency) and a power law above this frequency. It has been shown that the variability of this type can be produced by the inward diffusion of the local driving perturbations in a bounded configuration (accretion disk or corona). In the framework of this model, the perturbation diffusion time t_0 is related to the phenomenological break frequency, while the PDS power-law slope above the "break" is determined by the viscosity distribution over the configuration. The perturbation diffusion scenario explains the decay of the power of X-ray variability observed in a number of compact sources (containing black holes and neutron stars) during an evolution of these sources from low/hard to high/soft states. We compare the model predictions with the subset of data from Cyg X-1 collected by the *Rossi X-Ray Time Explorer* (*RXTE*). Our extensive analysis of the Cyg X-1 PDSs demonstrates that the observed integrated power P_x decreases approximately as the square root of the characteristic frequency of the driving oscillations $\nu_{\rm dr}$. The *RXTE* observations of Cyg X-1 allow us to infer $P_{\rm dr}$ and t_0 as a function of $\nu_{\rm dr}$. Using the inferred dependences of the integrated power of the driving oscillations $P_{\rm dr}$ and t_0 on $\nu_{\rm dr}$ we demonstrate that the power predicted by the model also decays as $P_{x,\rm diff} \propto \nu_{\rm dr}^{-0.5}$, which is similar to the observed P_x behavior. We also apply the basic parameters of observed PDSs, power-law indices, and low-frequency quasi-periodic oscillations to infer the Reynolds number (Re) from the observations using the method developed in our previous paper. Our analysis shows that Re increases from values of about 10 in low/hard state to about 70 during the high/soft state.

Subject headings: accretion, accretion disks — black hole physics — radiation mechanisms: nonthermal — stars: individual (Cygnus X-1)

1. INTRODUCTION

The main goal of the presented work is to explain a decay of the emergent time variability of X-ray emission in compact sources when these sources evolve from low/hard (LH) to high/soft (HS) states (see Remillard & McClintock [2006]; Titarchuk et al. [2007, hereafter TSA07], for details of observations). In particular, the power density spectrum (PDS) of black hole binaries in hard states is dominated by a component, which has a specific shape roughly described by a broken power law. The low-frequency part is mostly flat, while the power-law index α above the "break" frequency $\nu_{\rm br}$ is variable between 1 and 2. It is well established that the fractional rms variability in a source light curve decreases as a source evolves from LH state to HS state. Simultaneously, both $\nu_{\rm br}$ and α increase. Although empirical shot-noise models were able to describe in general the observed PDS shape (Focke et al. 2005), the physical picture explaining the observed evolution during spectral transitions was missing. Moreover, shot-noise models were challenged by the linear absolute rms-flux relation (Uttley et al. 2005; Uttley 2004). This rms flux relation assumes that amplitudes and timescales of shots are not independent, but are related in some way.

Lyubarskii (1997, hereafter L97), was the first to suggest a model for this time variability production in the accretion powered X-ray sources. He considered small-amplitude local fluctuations in the accretion rate at each radius caused by small-amplitude variations in the viscosity, and then studied the effect of these fluctuations on the accretion rate at the inner disk edge. His linear calculations show that if the characteristic timescale of the viscosity variations is everywhere comparable to the viscous (inflow) timescale, and if the amplitude of the variations is independent of radius, then the power spectrum of luminosity fluctuations is a power law $1/\nu$. If the amplitude of the variations increases with radius, the slope of the power spectrum of the luminosity variations is steeper than 1. Lyubarskii pointed out that he had no physical model for the cause of such fluctuations. Uttley et al. (2005) pointed out that rms-flux relation is naturally explained in the framework developed by Lyubarskii.

TSA07 formulated and solved the problem of local driving perturbation diffusion in a "disklike" configuration (which can be either a geometric thin Keplerian accretion disk or Compton cloud). The problem of the diffusive propagation of the space distributed high-frequency perturbations is formulated as a problem in terms of the diffusion equation for the surface density perturbations. This equation is combined with the appropriate boundary conditions. The formulation of this problem and its solution are general and classical. The parameters of the resulting PDS, diffusion timescale of the diffusion propagation of the local perturbations t_0 and the power-law index of the viscosity distribution over radius are essential parameters of diffusion in a given bounded configuration. In TSA07 we called our PDS model for the Green's function of the bounded configuration "white-red noise" (WRN), and we adopt this name throughout this paper.

The problem formulation in TSA07 was similar to L97's scheme. However, our method of finding the solution was

[1] George Mason University/Center for Earth Observing and Space Research, Fairfax, VA 22030; and US Naval Research Laboratory, Code 7655, Washington, DC 20375-5352; ltitarchuk@ssd5.nrl.navy.mil.

[2] Dipartimento di Fisica, Universitá di Ferrara, via Saragat 1, I-44100, Ferrara, Italy; titarchuk@fe.infn.it.

[3] Goddard Space Flight Center, NASA, code 661, Greenbelt, MD 20771; lev@milkyway.gsfc.nasa.gov.

[4] Goddard Space Flight Center, NASA/Universities Space Research Association, code 662, Greenbelt, MD 20771; nikolai@milkyway.gsfc.nasa.gov.

different. Lyubarskii treated the factorization of the driving term (i.e., separating it into two parts each depending on time and radius only) by linearizing the system. In TSA07 the analytical solution is obtained for the case of the factorized driving sources. Then, using the mean value theorem we showed that the general solution is simply a convolution of the configuration response signal (the Green's function) and the mean driving signal in the configuration. Thus, the resulting power spectrum of the X-ray signal, as a convolution, is a product of the power spectrum related to the configuration of the Green's function and that related to the perturbation sources (sources of driving oscillations).

The PDS of the Green's function is a WRN power spectrum. Specifically, the low frequency (LF) asymptotic form of the WRN PDS, when the frequency is less than the inverse of diffusion timescale in the disklike configuration t_0^{-1}, is characterized by a flat shoulder (white noise). In other words, the LF white noise shoulder is insensitive to the source and viscosity distributions over radius.

The high frequency (HF) asymptotic form of WRN is a power law $\nu^{-\alpha}$ with index α, which is determined by the viscosity and perturbation source distributions over the accretion configuration. The index is $\alpha = 3/2$ when the viscosity *linearly* increases with radius and the perturbation source's distribution is quasi-uniform. The basis of the presented power spectrum formation scenario is that the timing signal of the WRN PDS shape is a result of diffusive propagation of driving perturbations in the bounded configuration (disk or Compton cloud) in the same way that the X-ray photon spectrum is a result of the photon diffusion (namely, upscattering of seed photons) in the same bounded configuration.

The driving oscillation amplitude is assumed to be a smooth function of the radius. TSA07 suggested that driving fluctuations in the configuration can be introduced by g-mode driving oscillations at any given annulus. The local g-mode driving fluctuations, produced possibly by local Rayleigh-Taylor instabilities, are high-frequency damped quasi-periodic oscillations (QPOs) with frequencies that are related to the local Keplerian frequencies. As we mentioned above TSA07 formulated and solved a problem of the diffusive propagation of the space-distributed high-frequency perturbations in the bounded configuration. Our diffusion model for PDS is a product of the WRN PDS and the driving source PDS (Lorentzian).

The WRN PDS is a power spectrum of the solution of the initial value (Cauchy) problem, which is a linear superposition of exponential shots (see Wood et al. 2001). For example, if the driving perturbations are distributed according to the first eigenfunction of the diffusion operator, then the bounded medium works as a filter producing just one exponential shot as a result of the diffusive propagation of eigenfunction distribution of the seed perturbations. In the general case the resulting signal is a linear superposition of exponential shots which are *related* to the appropriate eigenfunctions. Furthermore, TSA07 demonstrated that *the observed rms-flux relations* (e.g., Uttley et al. 2005) are naturally explained by our diffusion model. In the framework of the linear diffusion theory the emergent perturbations are always linearly related to the driving source perturbations through a convolution of the configuration the Green's function and source distribution.

An important question is what our diffusion model predicts for relative contributions of the WRN PDS, the driving oscillation PDS in the resulting PDS, and for a dependence of the integrated PDS power on the driving oscillation frequency. The next question is how this model dependence of the integrated power versus the driving oscillation frequency is related to the observed dependence of that. The answers to these questions are the points of the presented study.

In § 2 we refer to details of Cyg X-1 observations with *RXTE*. In § 3 we outline the main features of the diffusion model and related formulas. In § 4 we show how the model integrated power versus the driving oscillation frequency fits X-ray data from Cyg X-1. In § 5 we present the inferred correlation of the Reynolds number with the driving oscillation frequency and the spectral state (photon index). Application of the paper results to the observed index-QPO frequency correlations is considered in § 6. Discussion and final conclusions follow in § 7.

2. OBSERVATIONS

For our analysis we used Cyg X-1 data from the Proportional Counter Array (PCA) and All-Sky Monitor (ASM) on board *RXTE* (Swank 1999).

The data are available through the GSFC public archive.[5] In this paper we present the analysis of a representative subset of *RXTE* observations of Cyg X-1. The reader can find the details of data reduction and analysis in Shaposhnikov & Titarchuk (2006) and TSA07. We chose approximately 200 observations to cover the complete dynamical range of the source evolution from the LH to the HS state. For the presented analysis we refit PDSs with our new model, and we use the results of our previous spectral analysis for photon index Γ.

To fit a PDS we used a sum of our perturbation diffusion model and one or two Lorentzians to account for the low-frequency quasi-periodic oscillations (LFQPOs). For higher photon indices, when the source is close to HS state, the contribution of the accretion disk variability component sometimes becomes significant. It is observed as an additional power law at lower frequencies (see TSA07 for details). We fit this component with a simple power law, when it is needed.

3. THE MAIN FEATURES OF THE MODEL AND UNDERLYING ASSUMPTIONS

We consider a scenario related to our model (see also TSA07) where the Compton cloud (disklike configuration) is located in the innermost part of the source and the Keplerian disk is extended from the Compton cloud (CC) to the optical companion (see Fig. 1 in Titarchuk & Fiorito 2004, hereafter TF04, for the model geometry). We remind the reader that the diffusion equation for the surface density perturbation is the same for any disklike configuration for which the rotational frequency $\Omega(R)$ as a function of radius R has a Keplerian-like profile, namely, $\Omega \propto R^{-3/2}$ (see Wood et al. 2001 for details). The standard Keplerian disk and ADAF kind of flow (Compton corona) are particular examples of these accretion disklike configurations.

The CC presumably contracts when the source goes to the softer state. TF04 inferred that the Compton cloud in LH state is about 40 Schzwarzchild radii (R_S), whereas that in HS state is about 4–5 R_S. It is obvious that the variability of the mass accretion rate in the cloud leads to the variability of the gravitational energy release there.

The Earth observer sees this mass accretion rate ($\dot{M}$) variation as a variability of X-ray flux coming from the source given that $\dot{M}$ regulates the supply of the soft seed photons upscattered off CC hot electrons. According to our scenario, in the equatorial plane the plasma is more dense and consequently colder than that in the CC outer parts. The soft photons are produced in these relatively cold equatorial layers of CC and then they are

[5] http://heasarc.gsfc.nasa.gov.

Comptonized off hot electrons of the CC outer part forming the resulting X-ray spectrum.

Thus, one can conclude that the variability of X-ray signal at energies higher than 3 keV (*RXTE* energy range) is mostly determined by the fluctuations of the luminosity $\Delta L_x(t)$ originated in the CC. Here we study the luminosity fluctuations $\Delta L_x(t)$ in the CC configuration.

We assume that the mass accretion rate variations $\Delta \dot{M}(0,t)$ are converted with efficiency $\varepsilon_{\rm eff}$ into the variations of the X-ray luminosity, i.e., $\Delta L_x(t) = \varepsilon_{\rm eff}\Delta \dot{M}(0,t)$. TSA07 showed that the fluctuation of the resulting X-ray oscillation signal $\Delta L_x(t)$ due to the diffusion of the driving perturbations is

$$\Delta L_x(t) = \int_0^t \varphi(t')Y(t-t')\,dt', \tag{1}$$

i.e., a convolution of the Green's function of the bounded configuration $Y(t)$ (WRN) and the source variability function $\varphi(t)$. The resulting power spectrum is

$$\|F_x(\omega)\|^2 = \left\|F_\varphi(\omega)\right\|^2 \|F_Y(\omega)\|^2, \tag{2}$$

where $F_x(\omega)$, $F_\varphi(\omega)$, and $F_Y(\omega)$ are Fourier transforms of $\Delta L_x(t)$, $\varphi(t)$, and $Y(t)$, respectively. The WRN PDS $\|F_Y(\omega)\|^2$ is described by equation (64) in TSA07 (also see the asymptotic forms of that in eqs. [65]–[66] there).

Using the total power of the driving oscillations $P_{\rm dr}$ one can present the driving oscillation PDS as (see eqs. [22] and [B5] in TSA07)

$$\left\|F_\varphi(\nu)\right\|_\nu^2 = \frac{\hat{\Gamma}_{\rm dr}P_{\rm dr}/(a\pi)}{(\nu-\nu_{\rm dr})^2+\left(\hat{\Gamma}_{\rm dr}/2\right)^2}, \tag{3}$$

where $\nu_{\rm dr} = \omega_{\rm dr}/(2\pi)$ is the driving oscillation frequency, $\hat{\Gamma}_{\rm dr}$ is a full width of half-maximum (FWHM) of the Lorentzian and a constant a varies in the range between 1 and 2 depending on the ratio of $2\nu_{\rm dr}/\hat{\Gamma}_{\rm dr}$:

$$a = 1 + \frac{2\arctan\left(2\nu_{\rm dr}/\hat{\Gamma}_{\rm dr}\right)}{\pi}. \tag{4}$$

For example $a = 1$ and 2 when $2\nu_{\rm dr}/\hat{\Gamma}_{\rm dr} \ll 1$ and $2\nu_{\rm dr}/\hat{\Gamma}_{\rm dr} \gg 1$, respectively.

It is worth noting that equations (1)–(4) were derived in TSA07 with an assumption that the local driving perturbations $\Phi(t,\xi)$ are damped quasi-periodic oscillations, namely,

$$\Phi(t,\xi) = A_\Phi f(\xi)\exp\left(-\frac{1}{2}\Gamma_{\rm dr}t + i\omega_{\rm dr}t\right), \tag{5}$$

where the amplitude of the driving oscillation is function of R only ($\xi = R^{1/2}$). Note the damping coefficients $\hat{\Gamma}$ in equation (3) and Γ in equation (5) are related as $\Gamma = 2\pi\hat{\Gamma}$.

Then TSA07 applied the mean value theorem for the integral $W(R,t)$ of equation (B2) in TSA07. Namely, the mean value theorem in its general form for the product of two continuos functions $g(t)$ and $f(t)$ states that if a function $g(t)$ is positive, i.e., $g(t) > 0$, then

$$\int_a^b g(t)f(t)\,dt = f(x)\int_a^b g(t)\,dt,$$

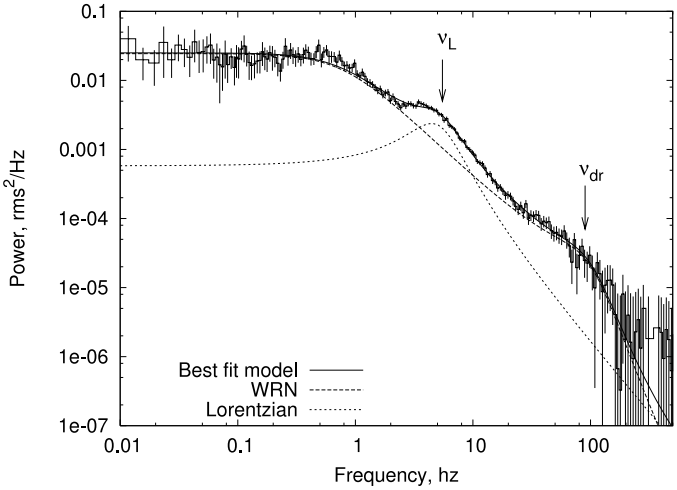

FIG. 1.—Particular example of observable PDS. The PDS continuum is fitted by our diffusion PDS model which is a product of WRN PDS and the driving oscillation Lorentzian. We also use a simple Lorentzian to fit QPO features.

where $a \le x \le b$. Given that the product of the Green's function $G(R,\xi,t)$ and the driving oscillation amplitude $f(\xi)$ in equation (B2) in TSA07 is positive we obtain that

$$W(R,t) = A_\Phi \int_0^t dt' \exp[-\Gamma_{\rm dr}t'/2 + i\omega_{\rm dr}(\xi_*)t'] \times \int_{R_{\rm in}}^{R_0} G(R,\xi,t-t')f(\xi)\,d\xi,$$

where $R_{\rm in} \le \xi_* \le R_0$. Then TSA07 proceeded with the Fourier transformation and PDS determination of $W(R,t)$, and ultimately they derived equations (1)–(4).

In Figure 1 we show a typical example of the model fit to the data using equation (2). The parameters of PDS continuum for WRN component $\|F_Y(\omega)\|^2$ (see TSA07 for details) are the diffusion timescale t_0, index of the power-law viscosity distribution ψ, and for the driving oscillation component $\left\|F_\varphi(\omega)\right\|^2$ they are $\nu_{\rm dr}$ and $\hat{\Gamma}_{\rm dr}$ (see eq. [3]).

The power-law index of the viscosity distribution ψ is related to the power-law index of the red noise in the WRN PDS (see TSA07):

$$\alpha = \begin{cases} \dfrac{3}{2} - \delta = \dfrac{16-5\psi}{2(4-\psi)} & \text{for } \psi > 0, \\ 2 & \text{for } \psi < 0. \end{cases} \tag{6}$$

The model-predicted integrated power is (see TSA07)

$$P_{x,\rm diff} \sim \frac{P_{\rm dr}}{2\pi\nu_{\rm dr}t_0(\mathcal{Q}+1/4\mathcal{Q})DC}, \tag{7}$$

where $\mathcal{Q} = \hat{\Gamma}_{\rm dr}/\nu_{\rm dr}$ is a quality factor for the driving signal and D is a factor of order of unity. Equation (7) was also derived using the mean value theorem for the integral of the product of two functions (see above). In TSA07 we assumed that a constant C related to the mean value of $\left\|F_\varphi(\nu)\right\|_\nu^2$ over the frequency integration range is about a few (see Appendix B2 in TSA07 for details). Here we specify and obtain the constant C when we compare the model dependence of $P_{x,\rm diff}$ on $\nu_{\rm dr}$ with the observable of P_x on $\nu_{\rm dr}$. In order to make this comparison one should determine the best-fit parameters t_0 and $P_{\rm dr}$ as functions of $\nu_{\rm dr}$. Note that to derive

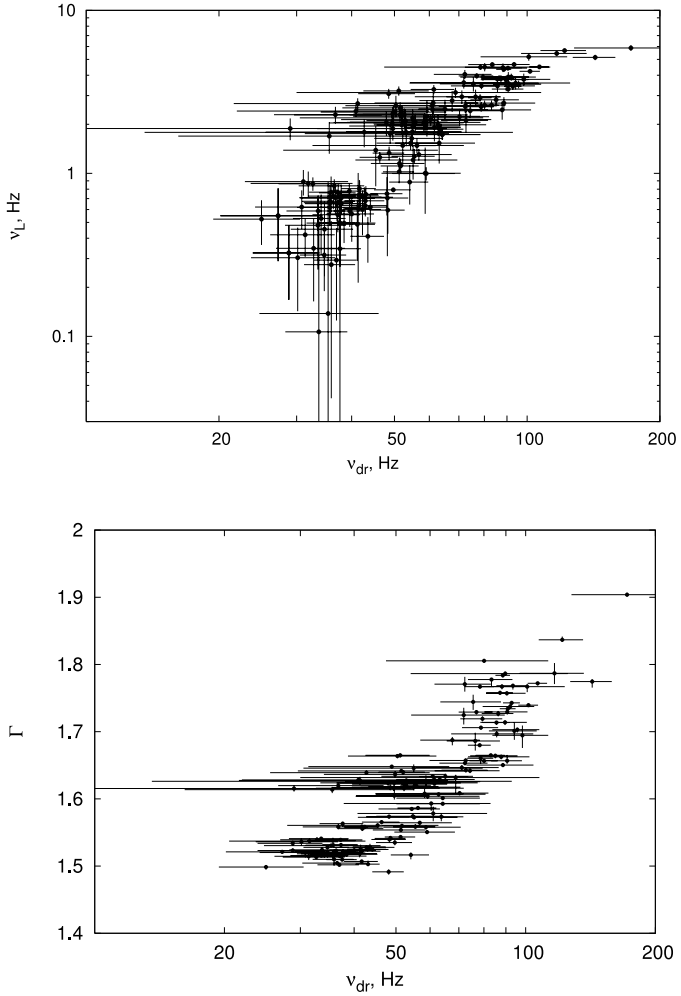

FIG. 2.—*Top*: Low QPO frequency ν_L vs. driving QPO frequency ν_{dr}. *Bottom*: Photon index Γ vs. ν_{dr}.

equation (7) we also use the fact that the WRN PDS $\|F_Y(\omega)\|^2$ is normalized to $1/(Dt_0)$, where $D \gtrsim 1$ (see eq. [B16] in TSA07).

Now we follow the method suggested in TSA07 to infer P_{dr} versus ν_{dr} from the observations. Namely, given the fact that the driving PDS is a constant at frequencies $\nu \ll \nu_{dr}$, we have

$$\left\|F_\varphi(\nu)\right\|_\nu^2 = \left\|F_\varphi(0)\right\|_\nu^2 = \frac{\hat{\Gamma}_{dr} P_{dr}/(a\pi)}{\nu_{dr}^2 + \left(\hat{\Gamma}_{dr}/2\right)^2}. \quad (8)$$

Because for any power spectrum $\|F(\omega)\|^2$,

$$\|F(\omega)\|^2 \, d\omega = \|F(2\pi\nu)\|^2 \, 2\pi \, d\nu = \|F(\nu)\|_\nu^2 \, d\nu,$$

we find that (compare with eq. [2])

$$\|F_x(\nu)\|_\nu^2 = (2\pi)^{-1} \left\|F_\varphi(\nu)\right\|_\nu^2 \|F_Y(\nu)\|_\nu^2. \quad (9)$$

Thus, a combination of equations (8) and (9) leads us to determination of the integrated power of the driving oscillations

$$P_{dr} = \frac{a\pi\left[\nu_{dr}^2 + \left(\hat{\Gamma}_{dr}/2\right)^2\right]}{\hat{\Gamma}_{dr}} \left\|F_\varphi(0)\right\|_\nu^2 = 2\pi^2 a \frac{\nu_{dr}^2 + \left(\hat{\Gamma}_{dr}/2\right)^2}{\hat{\Gamma}_{dr}} \frac{\|F_x(0)\|^2}{\|F_Y(0)\|^2}. \quad (10)$$

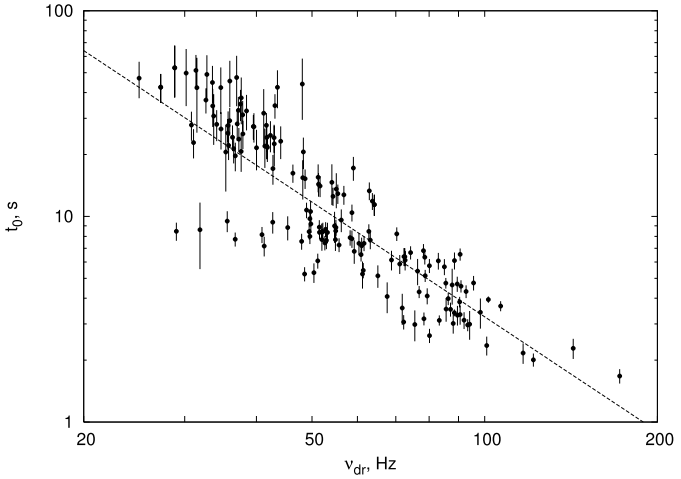

FIG. 3.—Best-fit model parameter, diffusion timescale t_0 vs. ν_{dr}. The dashed line is the best-fit power law $t_0 \propto \nu_{dr}^{-2.13\pm0.14}$.

We remind the reader that the values of ν_{dr} and $\hat{\Gamma}_{dr}$ are the best-fit PDS parameters, $\|F_x(0)\|^2$ is the observed PDS value at $\nu = 0$, and $\|F_Y(0)\|^2$ is a value of the normalized WRN PDS at $\nu = 0$. As we mentioned above, the integral of the normalized WRN PDS $\|F_Y(0)\|^2$ over ν is $1/(Dt_0)$.

4. THE INTEGRATED POWER VERSUS DRIVING OSCILLATION FREQUENCY AND PHOTON INDEX

In Figure 2 we present the observed correlation of low frequency QPO centroid ν_L with the driving QPO frequency ν_{dr} (*top*) and photon index Γ with ν_{dr} (*bottom*). These correlations imply that ν_L along with ν_{dr} increases when the source becomes softer. In other words, the emission area (CC) contracts when the source evolves to the soft states.

In Figure 3 we also see this effect of CC contraction as anticorrelation of the CC diffusion timescale t_0 with ν_{dr}. The inferred dependence of t_0 versus ν_{dr} can be fitted by the power law $t_0 \propto \nu_{dr}^{-2.13\pm0.14}$.

We infer the integrated power of the driving oscillations P_{dr} versus ν_{dr} (see eq. [10]), and then we obtain the model integrated power $P_{x,diff}$ versus ν_{dr} (see eq. [7]). In Figure 4 we show that the dependence of P_{dr} versus ν_{dr} can be fitted by the power law $P_{dr} \propto \nu_{dr}^{-1.8\pm0.16}$. Namely, the driving oscillation power P_{dr} decreases when the source (Cyg X-1) goes to softer states. Presumably, the decay of P_{dr} with ν_{dr} is also related to the contraction

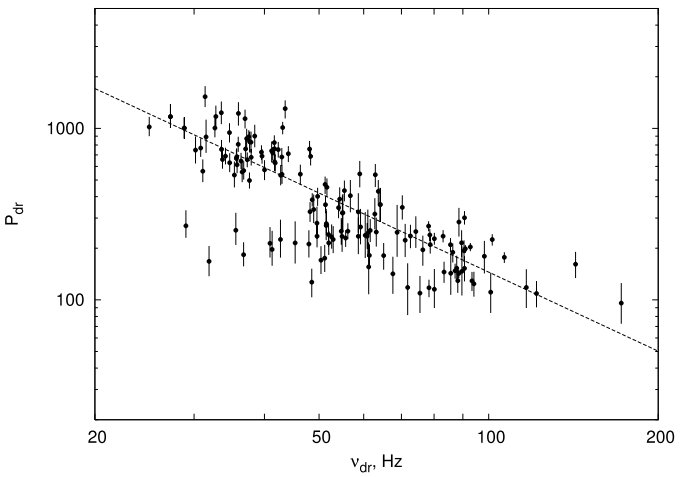

FIG. 4.—Inferred P_{dr} vs. ν_{dr}. The dashed line is the best-fit power law $P_{dr} \propto \nu_{dr}^{-1.8\pm0.16}$.

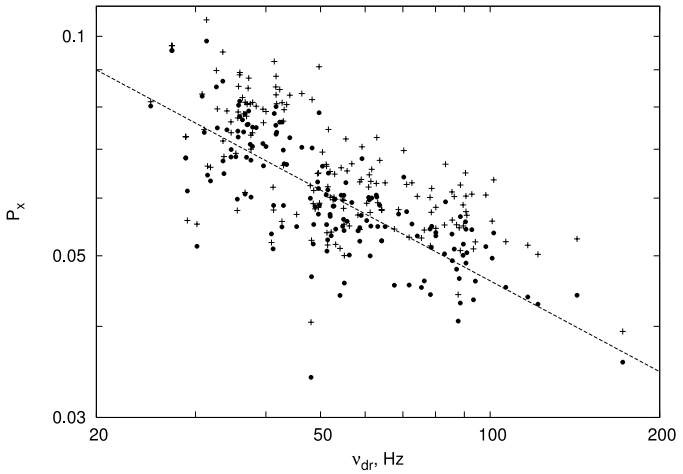

FIG. 5.—Comparison of the model $P_{x,\mathrm{diff}}$ vs. ν_{dr} (*plus signs*; using eq. [7]) with the observable P_x vs. ν_{dr} (*circles*). The dashed line is the best-fit power law $P_x \propto \nu_{\mathrm{dr}}^{-0.48\pm0.03}$.

of Compton cloud. The driving oscillations can result from the Rayleigh-Taylor (RT) local instability (see, e.g., Chandrasekhar 1961 and Titarchuk 2003). The decay of P_{dr} can be considered as a cumulative effect of the local RT instability when the effective area of a given configuration (CC) undergoing RT oscillations contracts.

In Figure 5 we present a comparison of the observable PDS integrated power P_x (*circles*) with the model predicted $P_{x,\mathrm{diff}}$ (*plus signs*; see eq. [7]). One can see that the dependence $P_{x,\mathrm{diff}}$ on ν_{dr} is similar to the observable correlation P_x versus ν_{dr}.

Note that we obtain the factor $C \sim 4$ (see eq. [7]) by shifting a set of the values of $P_{x,\mathrm{diff}}$ along the *Y*-axis, so that they fall on top of P_x values. The power law $P_x \propto \nu_{\mathrm{dr}}^{-0.48\pm0.03}$ fits the dependence of the theoretical and observable integrated powers versus the driving oscillation frequency.

5. THE REYNOLDS NUMBER OF THE ACCRETION FLOW IN COMPTON CLOUD CONFIGURATION

Titarchuk et al. (1998, hereafter TLM98) introduced the Reynolds number $\mathrm{Re} = V_R R/\hat{\nu}$ (γ in their notation), where V_R and $\hat{\nu}$ are an average radial velocity and an average viscosity over a given configuration, respectively, and R is a configuration scale. They demonstrate that the size of the transition layer (CC) between the fast rotating accretion disk and the relatively slow rotating central object (either BH or NS) strongly depends on the Reynolds number Re. It is worth noting that the α-viscosity parameter introduced by Shakura & Sunyaev (1973) is related to the TL (CC) parameter Re. Given that $\alpha \sim \hat{\nu}/(V_s H)$, where V_s is the sound velocity in the disklike configuration and H is a half of the configuration vertical size, we find that

$$\mathrm{Re} \sim \lambda/\alpha. \tag{11}$$

To infer this formula one should assume that $\lambda = H/R$ and $V_s \sim V_R$.

TSA07 has already shown that there is a possibility to infer Re, and consequently the α-parameter (see eq. [11]), using *RXTE* observations of BHs and NSs. This determination can be done if a particular *RXTE* PDS has the WRN component, and also if the QPO low frequency ν_L is present. TSA07 argue that the relation between observed frequencies ν_L and $1/t_0$ seen in Cyg X-1 PDSs is similar to the theoretical relation between the diffusion frequency ν_{diff} and the frequency of CC volume (magnetoacoustic) oscillations ν_{MA} (see, e.g., Titarchuk & Osherovich 1999). This fact leads them to conclude that ν_L can be considered as the frequency of the magnetoacoustic oscillations, a theory which was developed by Titarchuk et al. (2001, hereafter TBW01).

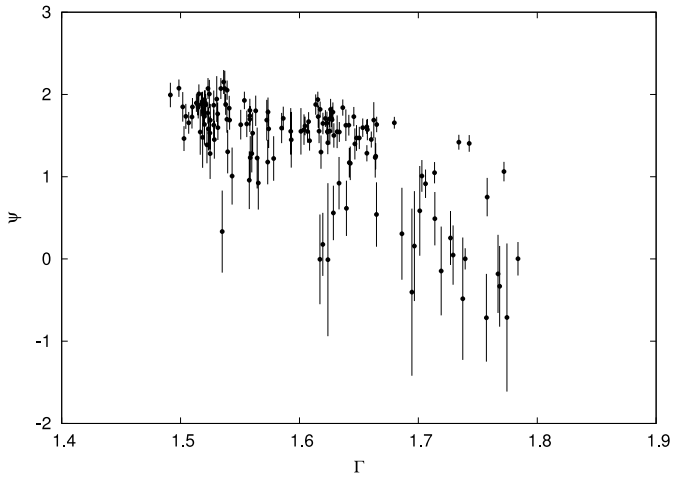

FIG. 6.—Best-fit index of the viscosity distribution ψ vs. Γ.

Using the best-fit parameters of the PDSs we can even infer the evolution of the Reynolds number of the accretion flow in the CC, with the change of photon index Γ. In fact, TSA07 relate diffusion time t_0 with Re and a magnetoacoustic QPO frequency ν_{MA} as

$$t_0 = \frac{4}{3}\frac{4}{(4-\psi)^2}\left[\frac{V_R R_0}{\hat{\nu}(R_0)}\right]\left(\frac{R_0}{V_R}\right) = \frac{4}{3}\frac{4}{(4-\psi)^2}\frac{\mathrm{Re}}{a_{\mathrm{MA}}\nu_{\mathrm{MA}}}, \tag{12}$$

where $V_R \sim V_s$ and a_{MA} is a numerical coefficient.

Formula (12) leads to the equation

$$\mathrm{Re} = 2\pi\left(\frac{a_{\mathrm{MA}}}{2\pi}\right)\frac{3}{4}\frac{(4-\psi)^2}{4}(\nu_L t_0), \tag{13}$$

which allows us to infer a value of Re using the best-fit model parameters t_0 and the QPO low frequency ν_L, which is presumably close to ν_{MA}. Ultimately, we can find the evolution of Re with the photon index Γ given that ν_L, t_0, and the viscosity index ψ evolve with Γ (see Figs. 2, 3, and 6).

In Figure 7 we present the inferred Reynolds number as a function of the photon index Γ. We use equation (13), and we set $a_{\mathrm{MA}} = 2\pi$ (see details of this determination of a_{MA} in TBW01

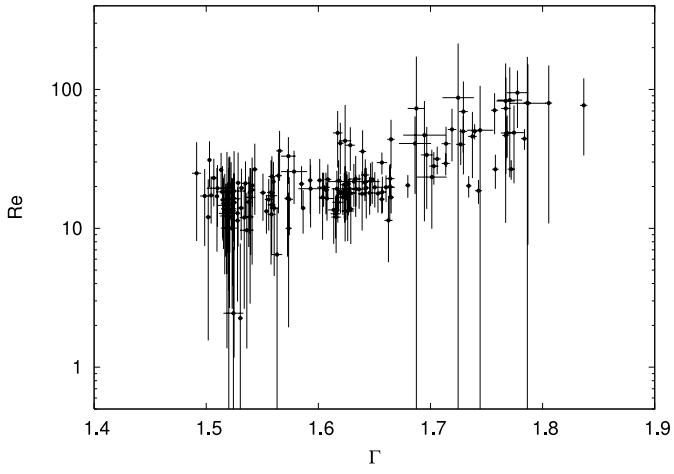

FIG. 7.—Inferred Reynolds number Re (using t_0, ν_L, ψ, and eq. [13]) vs. Γ.

and TSA07), and the observable correlations of ν_L and t_0 with Γ (see Figs. 2 and 3). One can see that Re steadily increases from 10 to 70 when the source evolves from the LH state to the HS state. In contrast, TSA07 found that Re $\sim 8 \pm 2.5$. We note, however, that in TSA07 only the WRN model was used without accounting for driving oscillation distribution, which significantly affects the resulting value for ψ. They also used a limited set of data.

Note the observed behavior of Re versus Γ and the mass accretion rate was predicted by TLM98, where they formulated a transition layer model (TLM) and studied its consequences for observations. It is important to emphasize that Re along with the photon index Γ, the low-frequency QPO ν_L, and the driving frequency $\nu_{\rm dr}$ can be considered as characteristics of the spectral state. All of them correlate with each other.

6. PHOTON INDEX–QPO FREQUENCY CORRELATION

TLM98 showed that the outer (adjustment) radius of the transition layer (CC) $R_{\rm out}$ measured in dimensionless units with respect to Schwarzschild radius $R_{\rm S} = 2GM/c^2$, $r_{\rm out} = R_{\rm out}/R_{\rm S}$, anticorrelates with Re or the photon index Γ (spectral state) only. Thus, ν_L (or $\nu_{\rm MA}$) as a ratio $\sim V_{\rm MA}/R_{\rm out}$ should correlate with Γ (or Re), where the values of ν_L related to the same Γ for different sources should be inversely proportional to a mass of the central object (black hole or neutron star). Note that a plasma velocity $V_{\rm MA}$ is also a function of Γ only. The comparison of the observed index–QPO frequency correlations for two different sources (with two different masses) should lead to determination of their relative masses with respect each other. This is the main idea behind the method of weighing black holes (TLM98) recently applied for BH mass determination in a number of Galactic and extragalactic sources (see TF04; Fiorito & Titarchuk 2004; Dewangan et al. 2006; Strohmayer et al. 2007; Shaposhnikov & Titarchuk 2007).

7. DISCUSSION AND CONCLUSIONS

Chakrabarti & Titarchuk (1995) proposed a model of the truncated Keplerian disk and hot corona located in the innermost part of the source using arguments in terms of radiation hydrodynamics. Churazov et al. (2001, hereafter CGR01), were the first who supported this model using the specific form of the power spectra of X-ray radiation. Particularly, they noted that two-component X-ray spectra (a soft multicolor blackbody and a harder power law) are frequently observed from accreting black holes. These components are presumably associated with the different parts of the accretion flow (optically thick and optically thin respectively) in the vicinity of the compact source. They also emphasized that for Cyg X-1, the overall shape of the power density spectra in the soft and hard spectral states can be *qualitatively* explained if the geometrically thin disk is sandwiched by the geometrically thick corona extending in a radial direction up to a large distance from the compact object. In the hard state the thin disk is truncated at some distance from the black hole followed by the geometrically thick flow. The break in the PDS is then associated with the characteristic frequencies in the accretion flow at the thin disk truncation radius.

However, there is a difference between CGR01's suggestions and the results of our paper. We come to the model of the truncated disk plus corona using the fit of the theoretical model of the power spectrum (see TSA07) to the data. Whereas CGR01 proposed a *qualitative* explanation of the data using Lyubarskii's idea on the formation of the power spectrum in X-ray binaries (see L97).

Our results confirm the CGR01 conclusion that a stable optically thick (but geometrically thin) disk extends down to small radii (as indicated by the strong and stable soft component), whereas prominent variations of the harder component (presumably related to Compton cloud) are present in the broad range of timescales (up to at least 10^2 s; see Figs. 2–3 in TSA07). We also confirm the observed emergent spectrum consisting of two components (soft stable component due to the disk emission and harder highly variable component due to Comptonization in the corona). The relative contribution of these two components to the luminosity of an averaged spectrum would then reflect the ratio of the energy releases in the disk and corona (or mass accretion rates). It is also worth noting that our presented analysis indicates that the high-frequency part of the PDS (QPO and turnover) at about 10 Hz and higher is possibly related to the local instabilities operating in the Comptonization region of the energy release (see CGR01). Note that Gierlinski & Zdziarski (2005) also pointed out the evolution of PDSs in XTE J15550−564 and XTE J1650−500. In particular, they showed a variable power in the Comptonized component (the PDS high-frequency component) when a given source evolves from hard to soft states.

However, there is a difference in the details between CGR01 and the results of our papers (see also TSA07). For example, the break in the PDS frequency range between 0.01 and 1 Hz is associated with the characteristic diffusion frequencies of the Compton cloud but not as that in CGR01 "with the characteristic frequencies in the accretion flow at the thin disk truncation radius."

Axelsson et al. (2005, hereafter ABL05), suggested a model of the PDS of Cyg X-1 which successfully presented a natural transition from hard state through intermediate state to soft state and back, and also allowed them to study the behavior of the Lorentzian components in detail. Using this model, consisting of a power law and two Lorentzian profiles, ABL05 were able to fit the Cyg X-1 PDSs, and to follow the components from hard state through the transitions and back. By choosing this simple empirical approach for the PDS data analysis, ABS05 could model the major features in all states with only three components. The parameters used in ABL05 were the width and peak frequency of the Lorentzians, along with the power at the peak frequency, The parameter evolution and its correlation between each other can all be described by continuous functions.

However, ABL05 did not address the nature of the components and continuum of the power spectrum. Their PDS description was purely phenomenological (compare with that in TSA07 and this paper).

ABL05 also showed that the PDS of Cyg X-1 is dominated by the same two Lorentzian components at all times. They came to this conclusion based on the fact that the relation of the peak frequencies of these Lorentzian components follows the pattern seen in both other BH and NS systems, and therefore they proposed that the physical processes responsible for them cannot be explained by invoking magnetic fields, a solid surface, or an event horizon.

It is worth noting that we also find that the diffusion (break) and QPO frequency follows the BH-NS pattern (see details in ST06 and TSA07). In addition to this we demonstrate that there is a certain correlation between QPO low frequency and driving (high) frequency and photon index (see Fig. 2) and show a correlation between the diffusion timescale (an inverse of the diffusion frequency) and the driving frequency (see Fig. 3). Furthermore, we explain the nature of the observational appearances of the power and photon spectra evolution by the evolution of the truncated disk and corona configurations when a

X-ray source evolves from hard state to soft states. We come to the conclusion that the truncated disk and corona scenario should be a common model in BH and NS systems.

In fact, TLM98 showed that the bounded configuration (Compton cloud) surrounding compact objects is the transition layer (TL) that is formed as a result of dynamical adjustments of a Keplerian disk to the innermost sub-Keplerian boundary conditions. They argued that this type of adjustment is a generic feature of the Keplerian flow in the presence of the sub-Keplerian boundary conditions near the central object, and that it does not necessarily require the presence or absence of a hard surface. TLM98 concluded that an isothermal sub-Keplerian TL between the NS surface and its last Keplerian orbit forms as a result of this adjustment. The TL model is general and is applicable to both NS and BH systems.

In conclusion, we want to single out the following:

1. We explain the decay of the emergent time variability of X-ray emission in compact sources when these sources evolve from low/hard to high/soft states. We find that the resulting power P_x from Cyg X-1 decays with the driving oscillation frequency $\nu_{\rm dr}$ as $P_x \propto \nu_{\rm dr}^{-0.5}$.

2. We show that the reciprocal of the diffusion timescale of the perturbation t_0^{-1}, the low-frequency QPO ν_L, and the driving oscillation frequency $\nu_{\rm dr}$, inferred by fitting the Cyg X-1 PDSs with our diffusion model, increase when the source evolves from low/hard state to high/soft state. This behavior of the PDS characteristics implies that the Compton cloud contracts toward softer spectral states. The driving oscillations are probably caused by the local Rayleigh-Taylor instability, in which cumulative $P_{\rm dr}$ decreases when the effective area of the configuration producing the RT oscillations contracts. The decay in driving power leads to the decay in the total observed variability power from the source. Using the facts that t_0^{-1}, ν_L, and $\nu_{\rm dr}$ increase with Γ and $P_{\rm dr}$, and P_x decreases with Γ, we conclude, as a result of our analysis, that the Compton corona shrinks when Cyg X-1 goes from the low/hard state to the high/soft state.

3. Our extensive data analysis of the power spectra from Cyg X-1 with an application of the method of Re determination developed in TSA07 indicates that Re related to Compton cloud configuration increases from values of about 10 in low/hard state to about 70 in high/soft state. We confirm the predictions by TLM98 that Re should increase with index and QPO frequencies. Thus, one can conclude that the observable index-QPO correlation is probably driven by the increase of Re when the source evolves from the low/hard state to the high/soft state. It is worth noting that inverse proportionality of the low-frequency QPO with respect to BH mass in the index-QPO correlation leads to the method of weighing BHs that employs this index-QPO correlation.

We acknowledge very useful comments and suggestions by the referee.

REFERENCES

Axelsson, M., Borgonovo, L., & Larsson, S. 2005, A&A, 438, 999 (ABL05)
Chakrabarti, S. K., & Titarchuk, L. 1995, ApJ, 455, 623
Chandrasekhar, S. 1961, Hydrodynamics and Hydromagnetic Stability (Oxford: Clarendon Press)
Churazov, E., Gilfanov, M., & Revnivtsev, 2001, MNRAS, 321, 759 (CGR01)
Dewangan, G., Titarchuk, L., & Griffiths, R. 2006, ApJ, 637, L21
Fiorito, R., & Titarchuk, L. 2004, ApJ, 614, L113
Focke, W. B., Wai, L. L., & Swank, J. H. 2005, ApJ, 633, 1085
Gierlinski, M., & Zdziarski, A. 2005, MNRAS, 363, 1349
Lyubarskii, Yu., E. 1997, MNRAS, 292, 679 (L97)
Remillard, R. A., & McClintock, J. E. 2006, ARA&A, 44, 49
Shakura, N. I., & Sunyaev, R. A. 1973, A&A, 24, 337 (SS73)
Shaposhnikov, N., & Titarchuk, L. 2007, ApJ, 663, 445
Shaposhnikov, N., & Titarchuk, L. 2006, ApJ, 643, 1098
Strohmayer, T. E., Mushotzky, R. F., Winter, L., Soria, R., Uttley, P., & Cropper, M. 2007, ApJ, 660, 580
Swank, J. H. 1999, Nucl. Phys. B, 69, 12
Titarchuk, L. 2003, ApJ, 591, 354
Titarchuk, L. G., Bradshaw, C. F., & Wood, K. S. 2001, ApJ, 560, L55 (TBW01)
Titarchuk, L. G., & Fiorito, R. 2004, ApJ, 612, 988 (TF04)
Titarchuk, L., Lapidus, I. I., & Muslimov, A. 1998, ApJ, 499, 315 (TLM98)
Titarchuk, L., & Osherovich, V. A. 1999, ApJ, 518, L95
Titarchuk, L., Shaposhnikov, N., & Arefiev, V. 2007, ApJ, 660, 556 (TSA07)
Uttley, P. 2004, MNRAS, 347, L61
Uttley, P., McHardy, I. M., & Vaughan, S. 2005, MNRAS, 359, 345
Wood, K. S., et al. 2001, ApJ, 563, 246 (W01)